Correlation between morphology with dynamic mechanical, thermal, physicomechanical properties and electrical conductivity for EVA–LDPE blends

I. Ray and D. Khastgir*

Rubber Technology Centre, Indian Institute of Technology, Kharagpur-721 302, India

(Received 29 April 1992; revised 20 August 1992)

Morphology, dynamic mechanical analysis, differential scanning calorimetry (d.s.c.), physicomechanical properties and electrical resistivity were studied on different blends of ethylene vinyl acetate (EVA) (28% VA content) and low density polyethylene (LDPE). An interpenetrating polymer network (IPN) is formed with a minimum of 50 wt% EVA in the blend. The glass transition temperatures change with blend compositions according to the Fox equation or the Gordon–Taylor relation. This indicates intermiscibility (compatibility). On curing, tensile strength goes up dramatically, and a maximum tensile value is obtained for 50:50 blend composition. The electrical resistivity of the blends is explained by a simple model, and can be correlated to morphology.

(Keywords: EVA–LDPE blends; dynamic mechanical analysis; differential scanning calorimetry; morphology; electrical resistivity)

INTRODUCTION

Judicious blending of two or more compatible polymers is the novel method for producing new materials having a unique set of properties. However, the term polymer–polymer compatibility is ambiguous in nature, and intermiscibility of polymers seems rather to be a clearer conception. To achieve the best optimization from a blend of two polymers, there should be some degree of mutual miscibility (compatibility).

Various techniques are available to investigate the compatibility or miscibility of polymers in blends. Such methods include differential scanning calorimetry (d.s.c.)[1–5], dynamic mechanical analysis (d.m.a.)[6–8], dielectric analysis (d.e.a.)[9–11], estimation of mechanical properties like tensile strength[12,13], and through optical methods like determination of the refractive index[14], dilatometry[15,16], morphological studies using scanning electron microscopy (SEM)[17,18], transmission electron microscopy (TEM)[19,20] techniques, density behaviour[21,22], etc.

From the concept of mixing of low molecular organic liquids, one can predict that the similarity in chemical structure and polarity may lead to the formation of a homogeneous mixture of two liquids without any stable interface. However, the situation is not exactly the same for high molecular weight polymers, where the molecular level of mixing from a thermodynamic point of view is excluded from reality. However, the problem of polymer–polymer miscibility becomes more severe when either or both of the components are partially crystalline[23].

The two polymers in the system under investigation here, namely the blends of ethylene vinyl acetate (EVA) with 28% VA copolymer and low density polyethylene (LDPE), have a structural similarity in the sense that the former is a copolymer of a non-polar methylenic chain ($-CH_2-$) with the polar acetate group, and the latter is a completely nonpolar methylenic chain. These two polymers differ in the degree of crystallinity, and also in their polarity. An attempt has been made to correlate morphological studies of these blends with d.s.c. and d.m.a. analysis, as well as with mechanical and electrical properties.

EXPERIMENTAL

Materials used

The materials used for the experiment and their characteristics are given in *Table 1*.

Preparation of the blends

Formulations of the blends are given in *Table 2*. The blends are designated as P_0, P_{30}, P_{50}, P_{70} and P_{100}, where the subscripts denote the weight per cent of LDPE in the blend. The blending was carried out in a Brabender Plasticorder PLE 330, using a cam-type rotor. The temperature of mixing was set at 130°C, and the rotor speed at 60 rev min^{-1}.

The mixes were compression moulded in a Moore press at a temperature of 170°C and a pressure of 100 ± 5 kg cm^{-2}.

* To whom correspondence should be addressed

0032-3861/93/102030-08

Table 1 Materials used in the investigation

	Trade name	Characteristics	Producer
EVA copolymer	PILENE 2806	28% VA content MFI = 6 g/10 min $d = 0.95$ g cm^{-3}	PIL, India
LDPE	INDOTHENE 20C A002	MFI = 0.2 g/10 min $d = 0.92$ g cm^{-3}	IPCL, India
Dicumyl peroxide	DCP	98% pure	Akzo Chemie, The Netherlands

Table 2 Formulation of the blends

	P_0	P_{30}	P_{50}	P_{70}	P_{100}
LDPE (g)	0	18	30	42	60
EVA (g)	60	42	30	18	0

Mechanical properties

Tensile properties were measured at room temperature (25°C), according to the ASTM D 412-80 test method, with a Zwick Universal Testing Machine (model 1445) with predetermined cross-head speed.

Differential scanning calorimetry

Differential scanning calorimetry of different blends and pure components was carried out using a Dupont thermal analyser-900. The scan was taken from −150°C to +150°C with a programmed heating rate of 20°C min^{-1} in a nitrogen atmosphere. The transition values were taken as the mid-point of the step or stair found in the curve of heat flow *versus* temperature.

To estimate the extent of strain-induced crystallization during tensile failure, the test pieces were preserved after tensile failure. Then, at a distance of 1 cm from the torn end, the samples were cut and collected for d.s.c. studies (*Figure 1*) (these are referred to as 'strained' samples later). These samples were subjected to d.s.c. studies, and compared with the results of original, unstrained samples to check the change in the enthalpy of fusion corresponding to the crystalline phase of individual polymers in the blend.

Dynamic mechanical analysis

Dynamic mechanical measurements were carried out on a dynamic mechanical analyser (Rheovibron DDV-III-EP). The experiment was performed in tension mode from −150°C to +150°C at a frequency of 3.5 Hz at 0.17% dynamic strain amplitude with a programmed heating rate of +2°C min^{-1}.

This measures the dynamic moduli (both storage and loss moduli) and damping (tan δ) of a specimen under oscillatory load as a function of temperature. In the text, the variation of tan δ with temperature for different compositions is discussed.

Morphology study

The intermiscibility of the constituent polymers in the blend was examined by studying the morphology with the help of a scanning electron microscope (Cam Scan Series model 2). Sheeted blend compositions were brittle fractured at cryogenic temperatures, and the fractured surface was subsequently etched by suitable solvents to selectively extract only the EVA phase. The solvent used was toluene, and the extraction process was allowed to continue for 24 h at about 40°C to reach the equilibrium condition. The solvent was removed from the sample later using vacuum extraction. The surface was then coated with gold and subsequently examined.

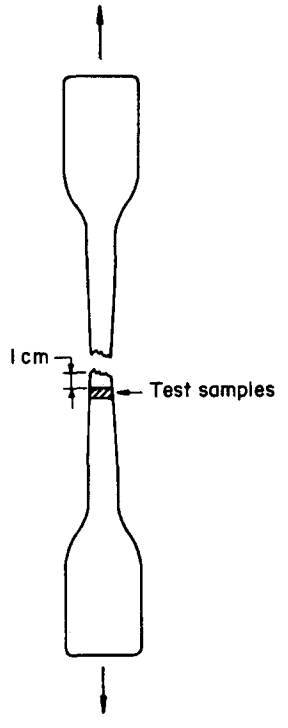

Figure 1 Schematic representation of sampling from the torn end of a tensile specimen for d.s.c. study

Electrical properties

D.c. volume resistivity of the sheeted materials was measured using a Hewlett Packard High Resistance Meter (model 4329 A).

RESULTS AND DISCUSSION

Morphology

The morphology of a melt-mixed two-component blend depends on the following factors:

(i) Component ratio
(ii) Intrinsic melt viscosity
(iii) Rate of shear during melt mixing and final moulding
(iv) Surface energy difference of the components.

Under identical processing conditions, the relative proportion of the components and their difference in melt viscosity play a significant role in determining the morphology[24]. If the individual polymers have similar melt viscosities, the resultant morphology of the blend is expected to be very fine, and a uniform distribution of the minor component in the major component becomes apparent. However, when the components have different melt viscosities, the morphology of the resulting blend depends on whether the minor component has a lower or a higher melt viscosity compared to the major one. If the minor component is of a lower viscosity, it will be finely dispersed in the matrix of the major component. The minor component will be coarsely dispersed, preferably in spherical domains, if its viscosity is higher

than that of the major one. In fact, the morphology should depend not only on dispersion (i.e. breakdown of an individual polymer phase into smaller domains), but also on the distribution of these domains in the matrix. The surface energy plays an important role during the process of distribution, specially modifiying the degree of coalescence of domains of the same components with each other.

The morphology of the EVA–LDPE blend shows marked deviation from observations made by Danesi and Porter[24] as evident from SEM photomicrographs of the preferential extraction of the EVA phase by suitable solvents from the blend. *Figures 2–4* show the morphology of P_{30}, P_{50} and P_{70} samples. The black domains indicate the positions of the extracted EVA phase. In the PE rich blend, P_{70}, having 30 wt% EVA, spherical, elliptical and elongated elliptical domains of EVA can be observed. There is also evidence of the coalescence of domains, leading to an uneven geometric shape. *Figure 4* also exhibits fine distribution of EVA particles in the continuous PE matrix, whereas a clear interpenetrating network (IPN) can be observed for the 50/50 EVA:LDPE blend (*Figure 3*). The channel-like co-continuous phases of both components running through one another forms the IPN. To establish the existence of an IPN, some samples of P_{50} blends were subjected to other, different solvents such as chloroform (shown in *Figure 5*) and butyl acetate (not shown), and SEM photographs were taken. It was found that, even after prolonged extraction of the EVA phase by different solvents, very similar interpenetrating structures are observed. However, in the P_{30} blend, where EVA is the major component, the co-continuity of both of the phases can still be observed. These variations in the domain morphology can be explained as follows.

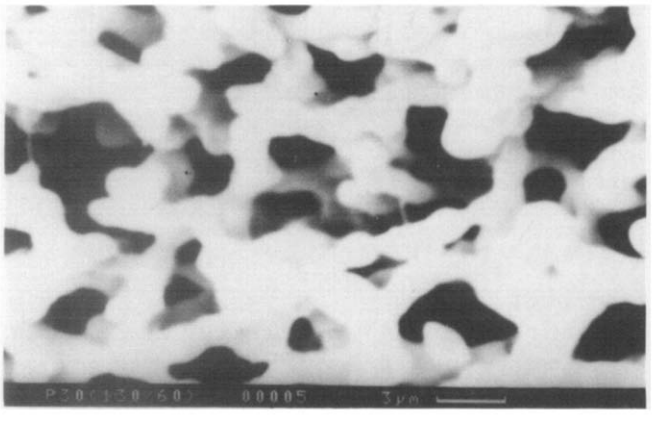

Figure 2 SEM photograph of solvent (toluene) extracted P_{30} blend (30/70 PE:EVA)

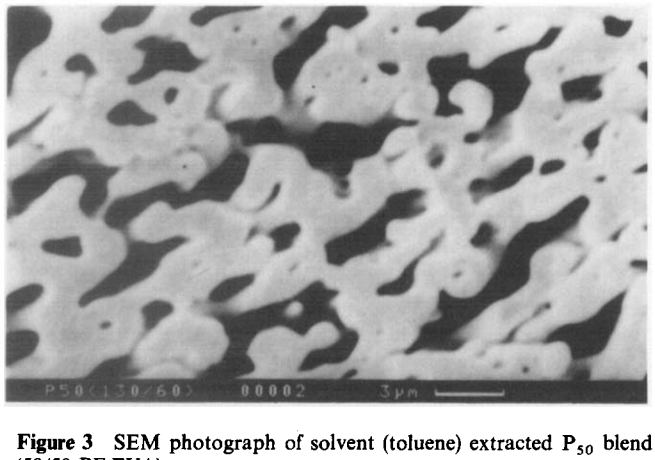

Figure 3 SEM photograph of solvent (toluene) extracted P_{50} blend (50/50 PE:EVA)

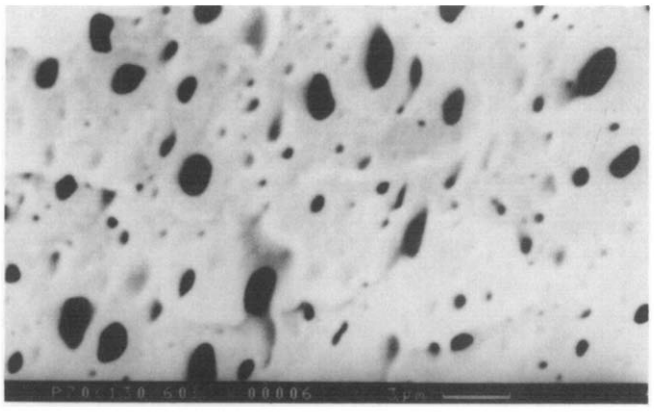

Figure 4 SEM photograph of solvent (toluene) extracted P_{70} blend (70/30 PE:EVA)

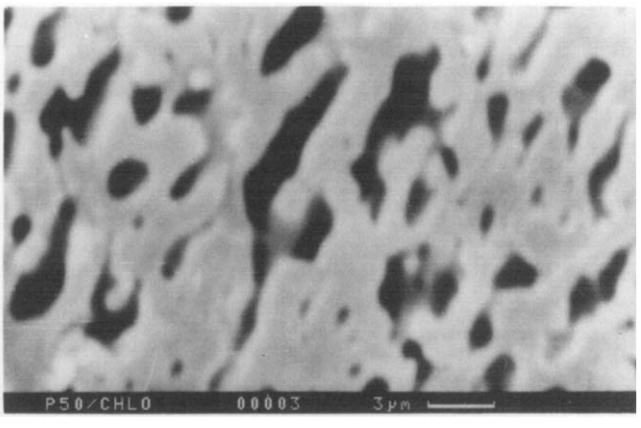

Figure 5 SEM photograph of solvent (chloroform) extracted P_{50} blend (50/50 PE:EVA)

The molten polymeric materials during melt-mixing experience a high shearing action. The induced shearing force deforms the dispersed molten polymer into elongated, rod-like particles, which constricts progressively until rupture. This constriction is mainly due to Brownian motion. Now, when the particles come out of the shearing zone, they may fully or partly relax to regain their original spherical, elliptical or elongated elliptical shapes, and may remain isolated from each other. However, there will be also a tendency for particle recombination leading to some intricate shape. The schematic diagram for this sort of shearing action, and subsequent reaction on the polymer domains, is given in *Figure 6*.

Dynamic mechanical analysis

Pure PE exhibits three different relaxation peaks, termed α, β and γ, where the α peak occurs at the highest temperature around 80°C, the β peak is for intermediate temperatures (−20°C), and the γ peak occurs at the lowest temperatures, around −120°C. The mechanism of α-relaxation is believed to be due to vibrational or reorientational motion within the crystals[25,26]. According to Takayangi[27], the α-relaxation is due to relaxation of $-CH_2-$ units in the crystalline region, and the molecular mechanism is the

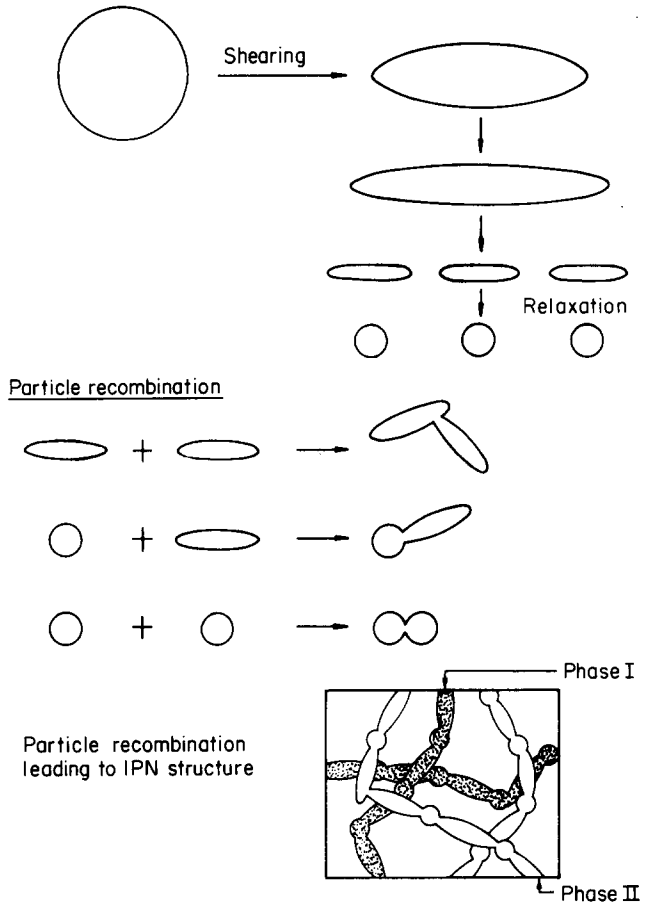

Figure 6 Schematic diagram of polymer domains under shearing action during melt-mixing and subsequent relaxation

same as the γ-relaxation at the lowest temperature which is associated with $-CH_2$ units for amorphous region. The temperature of α-relaxation depends on both side branch content, comonomer content like VA, and the method of crystallization and heat treatment[28–32]. The β-relaxation is associated with side branching of polyethylene. Oakes and Robinson[33] interpreted the β peak in LDPE as being due to the relaxation of branch points containing the side group –R, and this relaxation always occurs around the same temperature independent of whether R is methyl or another hydrocarbon group, or a chlorine atom or an acetate group, as found in EVA. The concentration of these side groups beyond a certain limit may affect the position of the β-peak. The γ-relaxation occurring at the lowest temperature is associated with the movement of methylene groups of the main chain in the amorphous region. This is also considered as the glass–rubber relaxation of the polymethylene group, which is the main backbone of PE[34].

EVA exhibits three different relaxations over the temperature range $+50$°C to -150°C. The highest relaxation temperature is at 47°C, and is associated with crystalline melting where there is a small tan δ peak but a sharp fall of storage modulus. The β transition occurs at -17°C in contrast to -25°C, as observed by others[29]. The relatively broad γ damping peak occurs around -135°C.

Thus, it shows that there is almost one-to-one correspondence in the existence of different types of peak for EVA and LDPE. The melt-mixed blends of EVA–LDPE also exhibit similar correspondence with either of the two pure components. The blend enriched with PE, P_{70}, shows γ, β and α peaks at around -127°C, -19°C and $+70$°C, respectively, whereas the EVA rich blend, P_{30}, exhibits γ (-133°C), β (-17°C) and α (62°C) transitions, as well as some kink due to crystalline melting of EVA at around 40°C. It is interesting to note that even after melting of the major EVA component in the P_{30} composition, the α-peak associated with the crystalline phase of PE could be identified. This is mainly because of co-continuity of the PE phase in P_{30}, as shown by the SEM photomicrograph (*Figure 2*) discussed earlier. Different damping peaks for the P_{50} blend containing equal proportions of EVA and LDPE are found at 78°C, -17°C and -131°C for α-, β- and γ-transitions, respectively. The plots of tan δ *versus* temperature are shown in *Figure 7*.

Three different peak temperatures, α, β and γ, for different compositions are presented in *Table 3*. The applicability of the Fox and the Gordon–Taylor relations described in equations (1) and (2) are verified for all compositions:

$$\frac{1}{T_g} = \frac{W_a}{T_{ga}} + \frac{W_b}{T_{gb}} \quad (1)$$

$$T_g = W_a T_{ga} + W_b T_{gb} \quad (2)$$

where T_{ga} and T_{gb} are the glass transitions of polymers *a* and *b*, T_g is the glass transition of the blend, and W_a and W_b are the weight fractions of *a* and *b* in the blend. It is to be noted that equation (2) is a special form of the Gordon–Taylor relation, which is applicable when the ratio of expansivity increments (k) of the two components

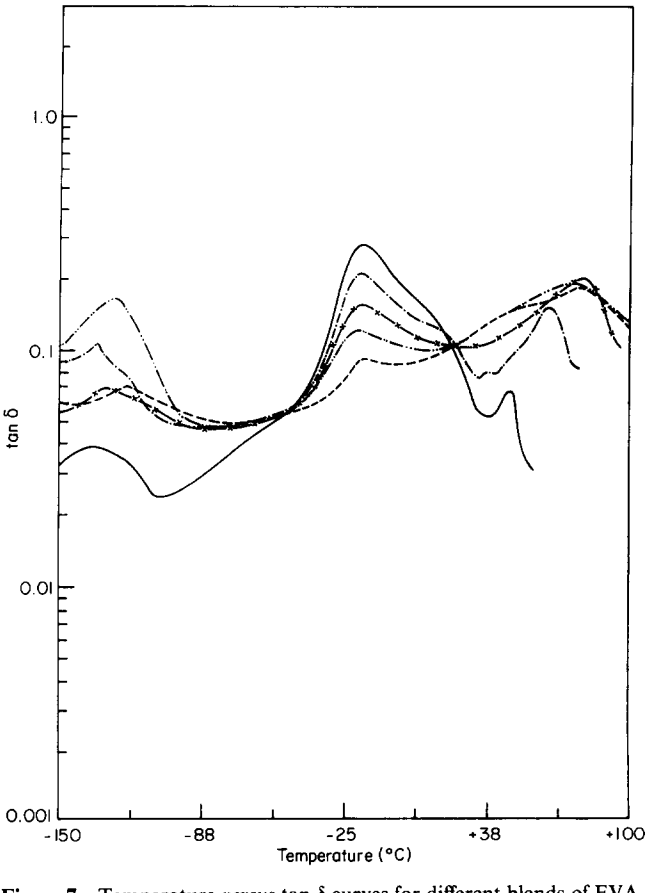

Figure 7 Temperature *versus* tan δ curves for different blends of EVA and LDPE: (——) P_0; (–·–) P_{30}; (–×–) P_{50}; (–···–) P_{70}; (– – –) P_{100} (see *Table 2* for details of blends)

Table 3 Transition temperatures from dynamic mechanical analysis

Sample reference	P_0	P_{30}	P_{50}	P_{70}	P_{100}
			(in °C)		
γ-transition temperatures (experimental)	−135	−133	−131	−127	−121
γ-transition temperatures (theoretical)	–	−131	−129	−125	–
β-transition temperatures	−17	−17	−17	−19	−20
α-transition temperatures	47	62	78	70	80

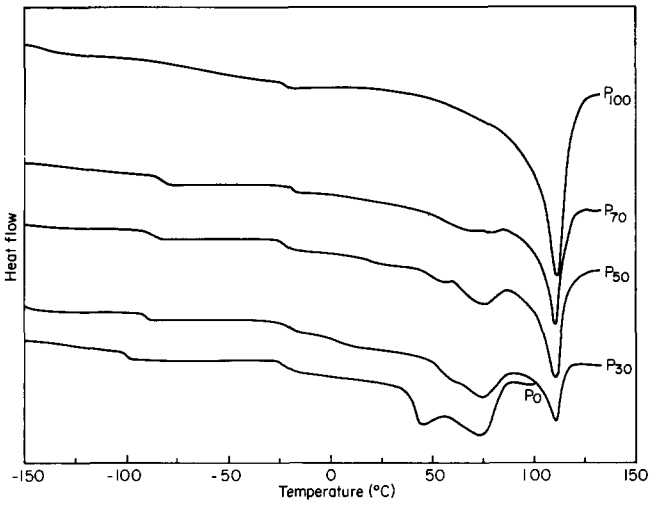

Figure 8 D.s.c. thermograms of different blends (see *Table 2* for details of blend compositions)

at their respective T_gs has a numerical value of unity. This condition would appear to hold experimentally when the difference between T_{ga} and T_{gb} is small, as in the present case. Under these conditions, similar values of T_g for the blends can be predicted using both equations (1) and (2).

It is found that the validity of both the equations is well established for γ-transitions for all blends P_{30}, P_{50} and P_{70}. Theoretical γ-transition temperatures, as predicted for compatible blends (which may be considered as the glass transition temperature), are in close agreement with experimental transition temperatures for all blends (*Table 3*). This signifies that there is a good degree of mixing in the amorphous zone of the two polymers. According to Thomas and Sperling[35], the controlling factors of the IPN include some degree of compatibility of the polymers, interfacial tension, and IPN composition. So, it is to be expected that some degree of compatibility between the two constituent polymers in this blend series should be there.

D.s.c. study

The d.s.c. technique has been widely used in the study of polymer–polymer compatibility and the amount of crystallinity present in semicrystalline polymer blends. D.s.c. thermograms exhibit (*Figure 8*) the plots of heat flow *versus* temperature. Transitions are detected in such curves from the occurrence of discontinuity in the curves. γ-transitions of different blends and pure components can be detected within a temperature range of −100 to −80°C. However, γ-transitions for pure PE cannot be detected. This may be due to interference from the crystalline zone[36]. In fact, the glass transition temperature of different blends increases with the increase in PE concentration in the composition. The closeness of transition temperatures of the pure components seems to be a problem for the accurate detection of T_g[37]. This problem intensifies in the case of semicrystalline polymers like polyethylene, where the d.s.c. technique is not found to be a suitable method for T_g measurement[38]. However, β-transition can be detected more distinctly from d.s.c. thermograms. In fact, there is practically no change in β-transition with composition. However, α-transition as obtained from d.m.a. studies cannot be detected in d.s.c., which coincides with the crystalline melting process. *Table 4* shows the different transition temperatures as obtained from d.s.c. studies. The difference between the γ-transition temperatures obtained by d.s.c. and d.m.a. is mainly because of the different heating rates used in these two measurements (heating rate for d.s.c. is 20°C min^{-1}, and that of d.m.a. is 2°C min^{-1}). Moreover, there is a difference in the technique; d.m.a. measures the damping characteristics due to the actual movement of the polymeric chains in the glass–rubber transition region, whereas in the d.s.c. measurements the discontinuity in the heat flow is associated with a sudden increase of the free volume due to molecular movements. However, d.m.a. measurements are more reliable due to their better reproducibility compared with d.s.c.

Blending two semicrystalline polymers like EVA and LDPE exhibits two distinct endothermic peaks corresponding to the melting of two different crystallites present in the blend. The existence of two melting peaks for each blend, which coincide exactly with peaks corresponding to two pure components, eliminates the probability of the intermiscibility of the crystalline phases of two polymers. The polymers may be intimately mixed in the molten state, but as the blends are cooled from the melt, the crystallization of different components occurs separately, leading to two distinctly different crystalline phases.

Physicomechanical properties

The measurement of mechanical properties like tensile strength is often used as a tool to predict the compatibility of a polymer blend. Compatible blends have been reported to exhibit a small maximum in the tensile strength *versus* composition curve over certain blend compositions[12]. The synergistic effect on tensile strength may be due to some strong specific interaction that leads to better molecular packing, which sometimes can be realized from higher densities of blends than the

Table 4 Transition temperatures from d.s.c.

Sample reference	γ-transition temperature (°C)	β-transition temperature (°C)
P_0	−100	−22
P_{30}	−90	−22
P_{50}	−86	−21
P_{70}	−82	−19
P_{100}	–	−23

calculated weight average densities of constituents. In contrast, blends of incompatible polymers have been reported to exhibit a broad minimum in tensile strength against the composition curve. So, tensile strength *versus* composition may be used as a relative indication of blend homogeneity. For the present system, we do observe a very narrow minimum in the tensile strength *versus* composition curve at around 70 wt% EVA concentration. The existence of minima in tensile strength *versus* composition curves is found even for different strain rates (*Figure 9*). The sharpness of minima increases with the decrease in strain rate. The stress–strain curves of different compositions at a fixed strain rate is presented in *Figure 10*. The stress–strain curves can be divided into three regions: (i) the Hookian region, where stress varies linearly with strain; (ii) the region of chain slippage, where a large increase of strain with a marginal change in stress occurs; and (iii) the region of strain hardening, where stress increases progressively with the increase in strain. The effect of the strain rate on the stress–strain behaviour of different blends has been detailed elsewhere by the present authors[39]. It is found that with the decrease in strain rate there is an increase in the degree of strain hardening. The effect becomes more pronounced as EVA concentration increases in the blend. However, it is interesting to note that both the phases in all blend compositions contribute to load bearing. Strain hardening is associated with the change in the degree of crystallinity of the sample, which can be detected by the increase in the enthalpy of the crystalline melting zone from a d.s.c. thermogram for a 'strained' sample compared to an unstrained one. From d.s.c. studies on strained samples, it has been found that there is an increase in the endothermic peak area corresponding to both of the components in the blend (*Figure 11*). The heat flow ordinate in *Figure 11* refers to equal masses of strained and unstrained samples.

This may be explained as follows: the effect of strain hardening is mainly due to strain-induced crystallization of amorphous phases of semicrystalline polymers, and the effect is more prominent for EVA, which contains a higher amorphous zone compared to LDPE. Where both the phases become continuous and form an IPN structure, the total load is borne by both the phases. Intimate mixing of two polymers in the amorphous regions leads to mutual load-sharing, even when one phase is not continuous.

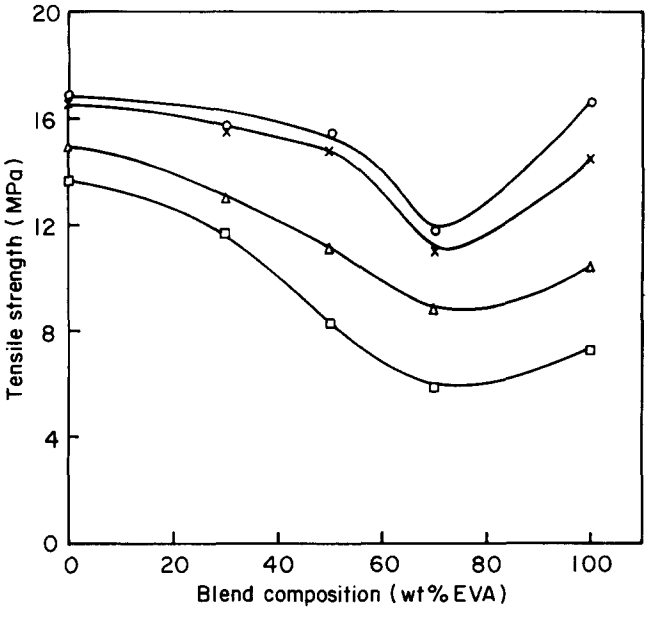

Figure 9 Tensile strength *versus* composition curves of EVA–LDPE blends at different strain rates: (○) 10 cm min^{-1}; (×) 20 cm min^{-1}; (△) 50 cm min^{-1}; (□) 100 cm min^{-1}

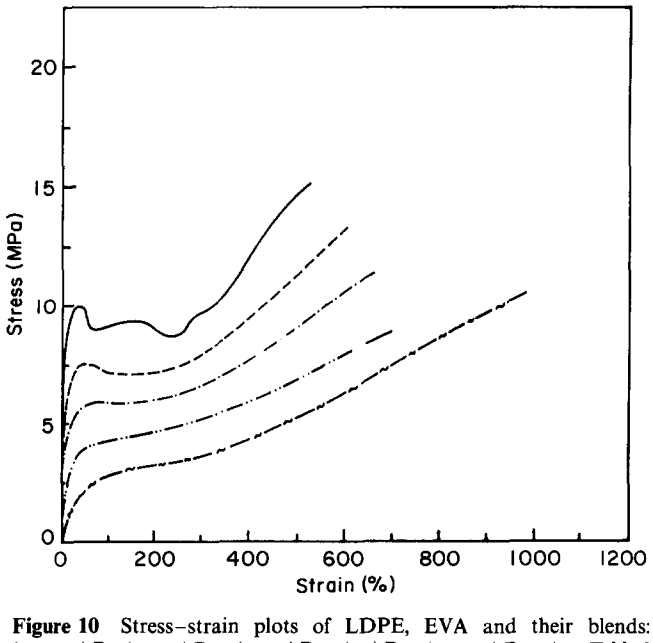

Figure 10 Stress–strain plots of LDPE, EVA and their blends: (—~—) P_0; (—··—) P_{30}; (—·—) P_{50}; (---) P_{70}; (———) P_{100} (see *Table 2* for details of blends). Strain rate = 50 cm min^{-1}

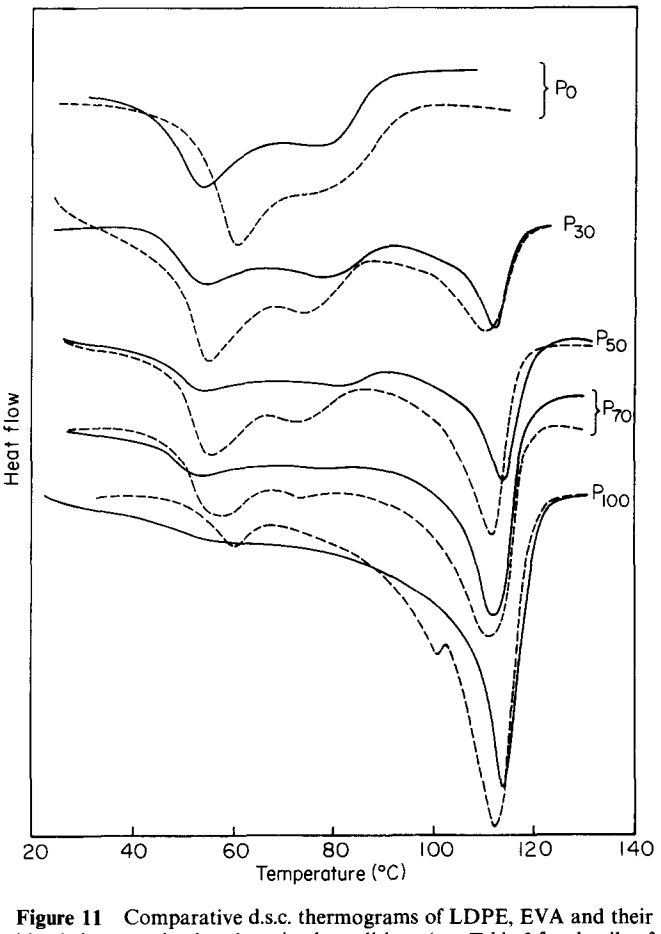

Figure 11 Comparative d.s.c. thermograms of LDPE, EVA and their blends in unstrained and strained conditions (see *Table 2* for details of blends)

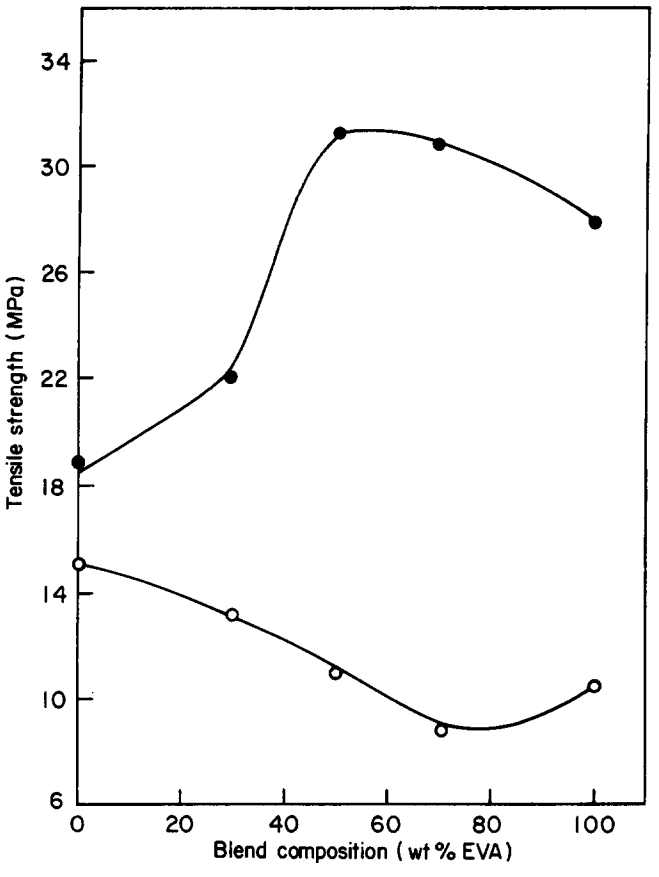

Figure 12 Tensile strength *versus* composition curve of cured blends (●) and uncured blends (○) at the same strain rate (50 cm min^{-1})

However, the benefit of an IPN structure cannot be realized unless the systems are cross-linked. When the two phases are stitched together through cross-linking, with the aid of a curing agent (php DCP), a dramatic improvement in tensile strength is observed. The tensile strength *versus* composition curves exhibit a maximum for a 50:50 blend composition, followed by a marginal change with a further increase in the EVA concentration in the blend (*Figure 12*). The interchain cross-linking improves the tendency of strain hardening of the system through lowering the probability of failure due to chain slippage, whereas the effect of cross-linking provides a marginal improvement in the PE phase. But the best property is achieved for the P_{50} blend which has a well-defined IPN structure, and is mainly due to interfacial cross-linking between PE and EVA.

Electrical resistance

The variation of conductivity with composition can be correlated with the morphology of the blend. The present blend system consists of two constituent polymers, LDPE having very high resistivity in the order of 10^{18} Ω-cm, the other constituent EVA being polar and comparatively more conductive, having a resistivity of the order of 10^{14} Ω-cm. For determination of the theoretical conductivity of any blend composition, the two constituents can be considered as two separate resistances. For co-continuous systems, for example where EVA concentration is ≥ 50 wt% in the composition, the following model can be postulated. When both the phases are continuous in the system, the resistivity of the blend is a parallel combination of the individual resistivities (*Figure 13a*), and is given by the formula:

$$\frac{1}{R_{\text{blend}}} = \frac{1}{R_{\text{PE}}} + \frac{1}{R_{\text{EVA}}}$$

For 30 wt% EVA composition, P_{70}, where EVA may be considered as discontinuous and distributed in the PE matrix, the following model can be postulated, as shown in *Figure 13b*.

The resistivity of the blend system according to this model can be represented as:

$$\frac{1}{R_{\text{blend}}} = \frac{1}{R_{\text{PE}}} + \frac{1}{R_X}$$

where $R_X = R_{\text{PE}} + R_{\text{EVA}}$.

It is found that the theoretically calculated resistivities are in close agreement with the experimentally observed ones (*Figure 14*). A deviation is observed only for the P_{70} blend – where experimental resistivities are found to be lower than those of theoretically calculated values. The

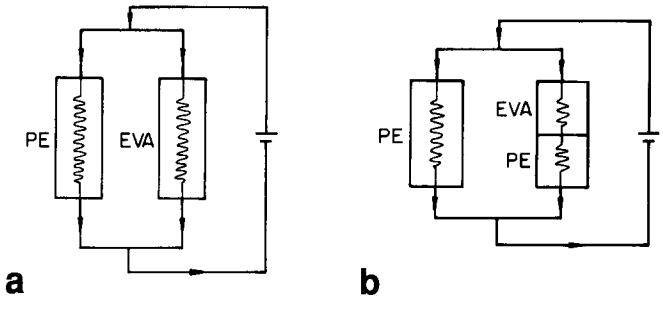

Figure 13 (a) Parallel combination of resistances in co-continuous matrices like 70/30 and 50/50 EVA:PE compositions in electrical resistivity measurements; (b) 30/70 EVA:PE composition showing series-cum-parallel combination of resistances in electrical resistivity measurements

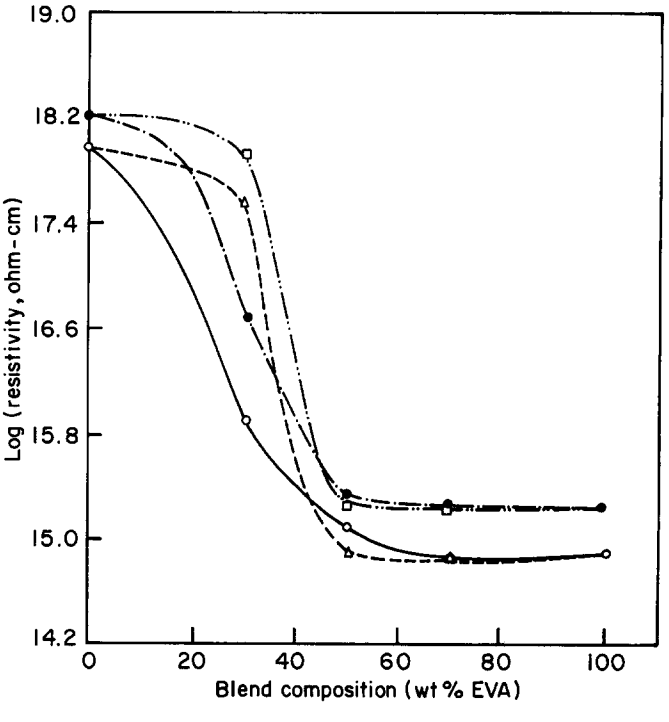

Figure 14 Theoretical and experimental curves of electrical resistivity *versus* blend compositions at 250 V and 1000 V: (□) theoretical curve for 250 V; (●) experimental curve for 250 V; (△) theoretical curve for 1000 V; (○) experimental curve for 1000 V

probable reason, even if the EVA phases are not visibly continuous, may be that a finer distribution of EVA domains throughout the matrix provides a relatively low resistance conducting path. The discontinuous region in such a conducting path may be small enough so that charge carriers can hop these gaps easily. And this is further shown by the fact that when measurements were carried out at higher voltages, say 1000 V, the resistivity of the sample was found to be lower. Higher voltages cause higher excitation, leading to a higher tendency to hop.

CONCLUSIONS

The blend morphology reveals the formation of an IPN structure for blends containing 50 and 70 wt% EVA. A blend containing 30 wt% EVA exhibits dispersion of the EVA phase in a continuous matrix of PE.

The miscibility of two polymers in amorphous zones is established from d.m.a. and d.s.c. studies. The existence of two distinct crystalline melting peaks in d.s.c. corresponding to two different crystallites reveals that the crystalline phases of individual components retain their respective identities. However, it is found that load is borne by both the components when subjected to stress. The morphology of different blend compositions can be correlated with their electrical conductivity; a 50:50 EVA–PE blend shows the maximum tensile strength through interfacial cross-linking. Further increase in EVA concentration causes marginal change in tensile strength.

ACKNOWLEDGEMENTS

The authors are grateful to the Department of Science and Technology, Government of India and Polyolefin Industries Ltd, India for funding this project.

REFERENCES

1 Nishi, T. and Wang, T. T. *Macromolecules* 1975, **8**, 909
2 Kwei, T. K., Patterson, G. D. and Wang, T. T. *Macromolecules* 1976, **9**, 780
3 de Boer, A. and Challa, G. *Polymer* 1976, **17**, 633
4 Schneier, B. *J. Appl. Polym. Sci.* 1974, **18**, 1999
5 Frisch, K. C., Klempuer, D., Migdal, S., Frisch, H. L. and Ghiradella, H. *Polym. Eng. Sci.* 1974, **14**, 76
6 Murayama, T. *J. Appl. Polym. Sci.* 1976, **20**, 2593
7 Marcincin, K., Ramanov, A. and Pollak, V. *J. Appl. Polym. Sci.* 1972, **16**, 2239
8 Secfried Jr, C. G. and Koleske, J. V. *J. Polym. Sci., Polym. Phys. Edn* 1975, **13**, 851
9 Feldman, D. and Rusu, M. *Eur. Polym. J.* 1974, **10**, 41
10 Wetton, R. E., MacKnight, W. J., Fried, J. R. and Karasz, F. E. *Macromolecules* 1978, **11**, 158
11 Mehra, U., Toy, L., Biliyar, K. and Shen, M. *Adv. Chem. Ser.* 1975, **142**, 399
12 MacKnight, W. J. and Karasz, F. E. 'Polymer Blends', (Eds D. R. Paul and S. Newman), Vol. 1, Academic Press, London, 1978, p. 187
13 Yee, A. F. *Polym. Prepr. Am. Chem. Soc. Div. Polym. Chem.* 1976, **17** (1), 145
14 Yuen, H. K. and Kinsinger, J. B. *Macromolecules* 1974, **7**, 329
15 Krause, S. and Roman, N. *J. Polym. Sci.* 1965, **A3**, 1631
16 Sperling, L. H., Taylor, D. W., Kirkpatrick, M. L., George, H. F. and Bardman, D. R. *J. Appl. Polym. Sci.* 1970, **14**, 73
17 Geil, P. *Ind. Eng. Chem., Prof. Res. Dev.* 1975, **14**, 59
18 Kaplan, D. S. *J. Appl. Polym. Sci.* 1976, **20**, 2615
19 McMaster, L. P. *Adv. Chem. Ser.* 1975, **142**, 43
20 Thomas, E. L. and Talmon, Y. *Polymer* 1978, **19**, 225
21 Noel III, O. F. and Carley, J. F. *Polym. Eng. Sci.* 1975, **15** (2), 117
22 Shwe, Y. J. and Ranby, B. *J. Appl. Polym. Sci.* 1975, **19**, 1337, 2143
23 Bohn, L. *Rubber Chem. Technol.* 1968, **41**, 495
24 Danesi, S. and Porter, R. S. *Polymer* 1978, **19**, 448
25 Rempel, R. C., Weaver, H. E., Sands, R. H. and Miller, R. L. *J. Appl. Phys.* 1957, **28**, 1082
26 McCrum, N. G., Read, B. E. and Williams, G. 'Anelastic and Dielectric Effects in Polymeric Solids', Wiley, London, 1967, p. 358
27 Takayanagi, M. *Mem. Fac. Eng. Kyushu. Univ.* 1963, **23**, 1
28 Schmieder, K. and Wolf, K. *Kolloid Z.* 1953, **134**, 149
29 Nielsen, L. E. *J. Polym. Sci.* 1960, **42**, 357
30 Nielsen, L. E. 'Mechanical Properties of Polymers', Reinhold, New York, 1962
31 Flocke, H. A. *Kolloid Z.* 1962, **180**, 118
32 McCrum, N. G., Read, B. E. and Williams, G. 'Anelastic and Dielectric Effects in Polymeric Solids', Wiley, London, 1967, p. 361
33 Oakes, W. G. and Robinson, D. W. *J. Polym. Sci.* 1954, **14**, 505
34 Willbourn, A. H. *Trans. Faraday Soc.* 1958, **54**, 717
35 Thomas, D. A. and Sperling, L. H. 'Polymer Blends', (Eds D. R. Paul and S. Newman), Vol. 2, Academic Press, London, 1978, p. 12
36 Koleske, J. V. and Lundberg, R. D. *J. Polym. Sci., Polym. Phys. Edn* 1969, **7**, 795
37 MacKnight, W. J. and Karasz, F. E. 'Polymer Blends', (Eds D. R. Paul and S. Newman), Vol. 1, Academic Press, New York, 1978, p. 197
38 MacKnight, W. J. and Karasz, F. E. 'Polymer Blends', (Eds D. R. Paul and S. Newman), Vol. 1, Academic Press, New York, 1978, p. 200
39 Roy, I., Khastgir, D. and Mukunda, P. G. *Angew. Makromol. Chem.* in press